Journal of The Electrochemical Society, **154** (3) G54-G57 (2007)
0013-4651/2007/154(3)/G54/4/$20.00 © The Electrochemical Society

Thermal Leakage Improvement by Using a High-Work-Function Ni Electrode in High-κ TiHfO Metal–Insulator–Metal Capacitors

K. C. Chiang,[a,z] C. C. Huang,[a] H. C. Pan,[b] C. N. Hsiao,[b] J. W. Lin,[a] I. J. Hsieh,[a] C. H. Cheng,[c] C. P. Chou,[c] A. Chin,[a] H. L. Hwang,[d] and S. P. McAlister[e]

[a]*Department of Electronics Engineering, Nano Science Technology Center, National Chiao-Tung University, University System of Taiwan, Hsinchu, Taiwan*
[b]*Instrument Technology Research Center, National Applied Research Laboratories, Hsinchu, Taiwan*
[c]*Department of Mechanical Engineering, National Chiao-Tung University, Hsinchu, Taiwan*
[d]*Department of Electrical Engineering, National Tsing Hua University, Hsinchu, Taiwan*
[e]*National Research Council of Canada, Ottawa, Canada*

An unavoidable drawback when using high-κ dielectrics in capacitors is the small bandgap and the related reduction in the band-offset, which results in a large leakage current at elevated temperatures. We report improvements in the thermal leakage current by using Ni as a high-work-function top electrode for high-κ TiHfO capacitors. This avoids sacrificing the overall κ value by using a multilayer or laminate structure and results in better voltage linearity, which is important for analog/radio frequency integrated circuits.
 [DOI: 10.1149/1.2422874]

Manuscript submitted August 17, 2006; revised manuscript received October 19, 2006. Available electronically January 5, 2007.

Metal–insulator–metal (MIM) capacitor development aims to achieve high-capacitance density devices using a simple integration process to yield multiple functions for system-on-chip (SOC) applications. The technological trend has been to increase the κ value in the dielectrics, from using Al_2O_3 and then HfO_2–Al_2O_3[1] and Nb_2O_5[2] to TiTaO[3-5] or TiHfO[6] (κ ≈ 45–50). However, one drawback for higher κ MIM devices is that the smaller bandgaps (E_G) result in a large leakage current at elevated temperatures, so that the stored charge leaks from the capacitor ($Q = CV$). This is also a challenge in flash memory[7] and is unavoidable during integrated circuit (IC) operation, where there is a large device density in the circuit and high dc power dissipation. A possible solution is to add a high E_G dielectric to form a multilayer[8,9] or laminate structure,[1] but the overall κ value and voltage coefficient of capacitance (VCC) are then degraded. In this paper we report the use of a high-work-function (ϕ_m) metal to reduce the leakage current, without sacrificing the capacitance density. By using high ϕ_m Ni (5.1 eV) for high-κ TiHfO capacitors, the leakage current at 125°C was reduced by nearly 2 orders of magnitude compared with control devices which used an Al electrode (ϕ_m = 4.1 eV). Economically it is also better to use Ni rather than Ir, which has been used previously in complementary metal oxide semiconductors (CMOSs).[9]

Experimental

The devices were fabricated by first depositing 2 μm SiO_2 on a Si wafer and then forming the lower capacitor electrode using physical vapor deposit (PVD)-deposited TaN/Ta bilayers. The Ta was used to reduce the series resistance and the TaN served as a barrier layer between the high-κ TiHfO and the Ta electrode. Then, the $Ti_xHf_{1-x}O$ ($x \approx 0.6$) dielectric was deposited by PVD, followed by a 400°C oxidation and an annealing step to reduce the leakage current. Finally, Ni or the control Al was deposited and patterned to form the top capacitor electrode. Devices of various sizes were made, and those measured were typically 20 × 20 μm in area. The fabricated devices were characterized by capacitance–voltage (C–V) and current-density–voltage (J–V) measurements using an HP4155B semiconductor parameter analyzer and an HP4284A precision LCR meter.

Results and Discussion

Electrical C–V and J–V characteristics.— Figure 1a shows the C–V characteristics at various frequencies for [Ni or Al]/TiHfO/TaN MIM capacitors having ~11 fF/μm^2 capacitance density. The Ni electrode devices show better frequency dispersion and voltage independence (small VCC) than those using Al. This indicates that the magnitude of the barrier height, ϕ_m, of the upper

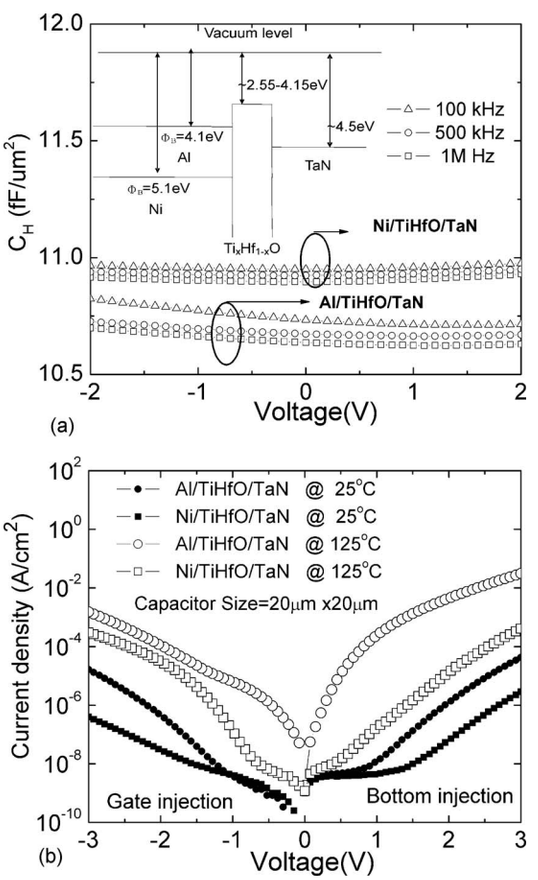

Figure 1. (a) C–V characteristic of [Ni or Al]/TiHfO/TaN capacitors measured at various frequencies and (b) J–V characteristics of [Ni or Al]/TiHfO/TaN capacitors measured at 25 and 125 °C.

[z] E-mail: gorden.ee91g@nctu.edu.tw

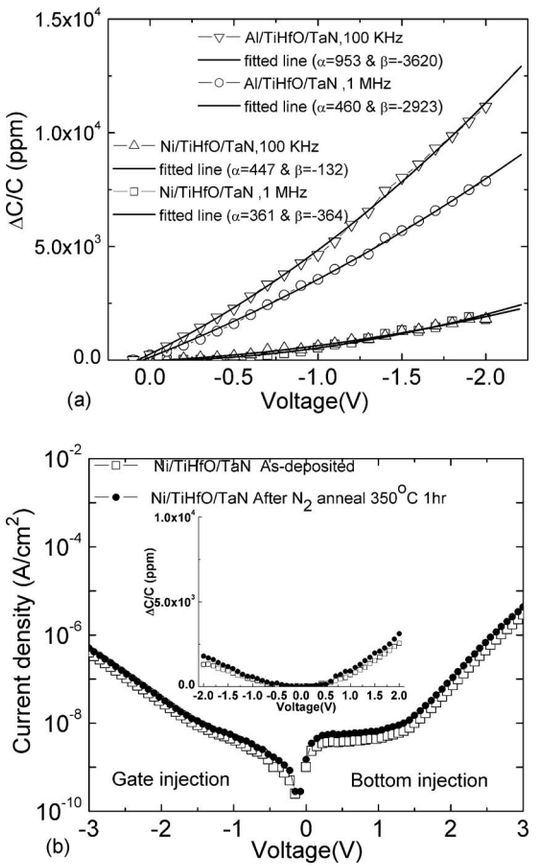

Figure 2. (a) Δ*C*/C–V characteristics of [Ni or Al]/TiHfO/TaN capacitors and (b) J–V and Δ*C*/C–V (insert) for the Ni-based capacitors.

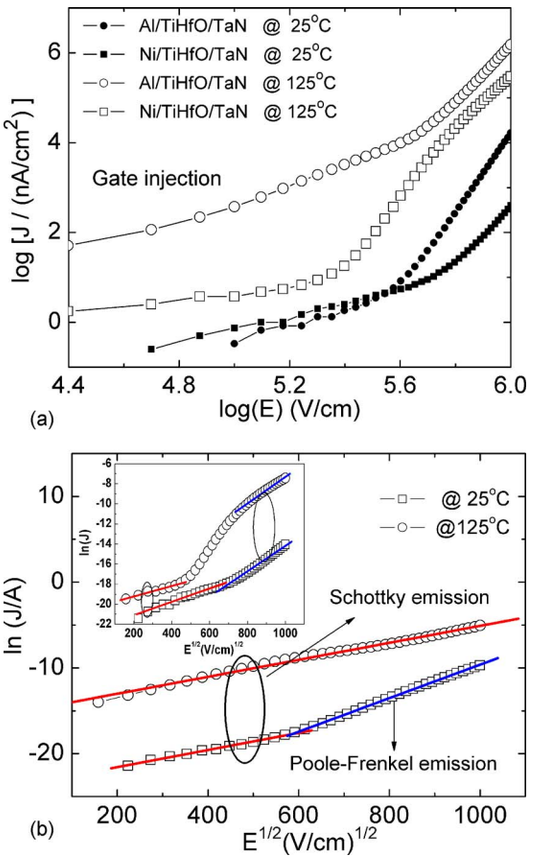

Figure 3. (Color online) (a) *log*(*J*) vs *log*(*E*) plots of [Ni or Al]/TiHfO/TaN capacitors measured at 25 and 125°C (b) Measured and simulated J–$E^{1/2}$ of an Al/TiHfO/TaN capacitor. A Ni/TiHfO/TaN device is shown in the inset.

electrode is important in improving the device performance. In Fig. 1b the J–V characteristics of the TiHfO MIM capacitors, measured at 25 and 125°C, show that the advantage of the Ni electrode is preserved at the higher temperature, even though the leakage currents are both increased exponentially.

ΔC/C and VCC α.— Capacitor voltage linearity is an important factor for MIM capacitors in silicon radio frequency (rf) and mixed-signal IC applications. This voltage dependence can be obtained by fitting the measured C–V characteristics using a second-order polynomial expression of the form

$$\Delta C(V) = C_0(\alpha V^2 + \beta V) \qquad [1]$$

Here C_0 is the capacitance at 0 V, and α and β represent the quadratic and linear voltage coefficients of capacitance, respectively. Because the effect of the linear β term can be compensated by appropriate circuit design (by using a differential method[10-13]), the α term is the main parameter for the voltage dependence. Figure 2a depicts the variation of $\Delta C(V)/C$ as a function of voltage for the [Ni or Al]/TiHfO/TaN capacitors at different frequencies. The lines in the figure are fits to the data using the expression above. The Ni top electrode not only reduces the leakage current but also improves the frequency dispersion, $\Delta C/C$, and α. This improvement of the voltage dependence may arise from the higher barrier height ϕ_m between the electrode and the dielectric, which leads to a lower carrier concentration.[14,15] In general, the dispersive behaviors, such as the voltage and frequency dependence, are believed to be related to the existence of bulk-dielectric traps near the dielectric/metal interface. Different traps induce charges with different time constants and strongly modulate the capacitor charges at certain frequencies. Therefore, when the applied frequency is high, VCC is low because the induced charges are unable to follow the ac signal.[2-6]

In addition, the stability of the devices after a thermal treatment of 350°C for 1 h was good, as indicated from the J–V and Δ*C*/C–V characteristics shown in Fig. 2b. This suggests that the devices are suitable for the fabrication of MIM structures in back-end-of-the-line (BEOL) processes.

Current conduction mechanism.— To investigate the large leakage-current difference for the [Ni or Al]/TiHfO/TaN MIM capacitors, an understanding of the conduction mechanism is necessary. This is also useful in the development of advanced MIM devices. According to the space-charge-limited current (SCLC) theory,[16-18] the J–V characteristics should initially be ohmic ($J \sim V$) at low applied bias. As the applied voltage is increased, a strong injection of the charge carriers into the bulk of the film occurs, giving $J \sim V^2$. Figure 3a shows the *log*(*J*) vs *log*(*E*) dependence. The slopes of the curves in both the low- and high-field regimes are not in agreement with the ohmic and SCLC mechanisms.

To investigate further, we have plotted *ln*(*J*) vs $E^{1/2}$ for Schottky emission (SE) or Frenkel–Poole (FP) conduction, as shown in Fig. 3b, i.e.,

$$J \propto \exp\left(\frac{\gamma E^{1/2} - V_b}{kT}\right) \qquad [2]$$

where

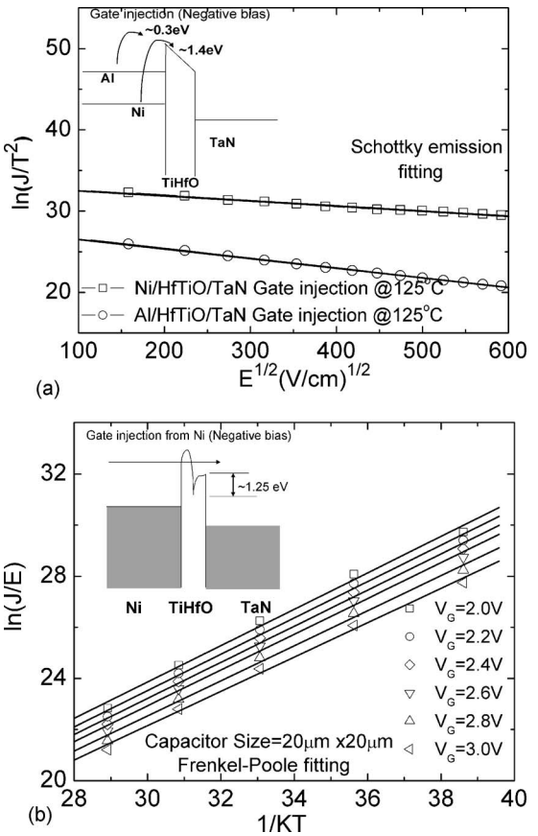

Figure 4. (a) SE fitting of [Ni or Al]/TiHfO/TaN capacitor data at low electric field and (b) FP fits of a Ni/TiHfO/TaN capacitor data at high field. The related band diagrams are included.

$$\gamma = \left(\frac{e^3}{\eta\pi\varepsilon_0 K_\infty}\right)^{1/2} \qquad [3]$$

The constant η is equal to 1 or 4 for the FP or SE cases. The fits to the experimental data give slopes γ of 1.65 or 3.32×10^{-5} eV $(m/V)^{1/2}$ for the SE or FP mechanisms, respectively, by using a refractive index $n = 2.45$ for $Ti_xHf_{1-x}O$ ($x \approx 0.6$).[19] This n value is consistent with a linear interpolation of the reported 2.57 value for TiO_2 and 1.85 for HfO_2.[20] The leakage current at 25°C for the Al electrode on TiHfO/TaN is consistent with an SE description at low field and FP at high field through a trap-conduction mechanism. However, the leakage at 125°C appears to be dominated by the SE process, due to the small energy barrier ϕ_b. In contrast, the leakage at 125°C for the Ni case is still governed by the SE and FP at low and high field, respectively, which is due to the large ϕ_b, as depicted in the figure insert.

Because the low-field conduction for both Ni and Al electrodes at 125°C is governed by SE, we have plotted the detailed $ln(J/T^2)$-$E^{1/2}$ relation in Fig. 4a to extract ϕ_b. A Schottky barrier height of 0.3 or 1.4 eV for Al/TiHfO or Ni/TiHfO was obtained, where the significantly larger ϕ_b using Ni accounts for the ~2 orders of magnitude lower leakage current, compared with devices using Al. From the extracted ϕ_b and the reported ϕ_m data, the conduction band of the dielectric with respect to the vacuum level is at 3.8 eV; this gives an E_G for $Ti_xHf_{1-x}O$ of 4.3 eV with $x \approx 0.6$. Because the conduction mechanism at high electric field for the Ni electrode on TiHfO is governed by an FP mechanism, we also plotted the $ln(J/E)$-$1/KT$ relationship in Fig. 4b. The extracted trap energy is 1.2 eV from the conduction band of TiHfO, as shown in the inserted plot. This value is less than the SE energy of 1.4 eV, which supports the contention that the high-field conduction should be described as an FP process rather than an SE one. This result also explains that the conduction mechanism for the low ϕ_m Al electrode case should be governed by SE because its SE barrier height is only 0.3 eV, whereas the FP case requires 1.2 eV. Thus, the use of a high ϕ_m electrode, such as Ni, is vital when using high-κ dielectrics which have small E_G values.

Performance comparison.— Table I summarizes the important device data for MIM capacitors with various high-κ dielectrics and work-function metals. The thermal leakage decreases with increasing ϕ_m of the metal electrode from Al to Ni. High ~11 fF/μm^2 density, small quadratic VCC α of 361 ppm/V^2, and low 1×10^{-7} A/cm^2 leakage current at 125°C were simultaneously measured in the Ni/TiHfO/TaN devices, which is comparable with or better than other reported data. The VCC α is strongly dependent on the capacitance density and electric field;[1-6,21-24] an exponential decrease of α with increasing capacitance effective thickness (CET), or $1/C$, was observed for all the capacitors, as shown in Fig. 5. The VCC α is also dependent on the specific high-κ dielectric, where Ta_2O_5 exhibits superior VCC compared with HfO_2 and Al_2O_3.[8] In addition, the metal-dielectric interface is also important for the VCC α and formation of such an interfacial layer degrades the capacitance performance.[23] Overall, MIM capacitors incorporating a

Table I. Comparison of device data for MIM capacitors with various high-κ dielectrics and work-function metals.

	HfO_2[21]	Tb–HfO_2[22]	Al_2O_3–HfO_2[1]	Nb_2O_5[2]	TiTaO[3]		This work	
Top metal	Ta	Ta	TaN	Ta	Ir	Ir	Ni	Al
Lower metal	TaN	TaN	TaN	Ta	TaN	TaN	TaN	TaN
C Density (fF/μm^2)	13	13.3	12.8	17.6	10.3	23	10.8	10.6
J (A/cm^2) at 25°C	6×10^{-7} (2 V)	1×10^{-7} (2 V)	8×10^{-9} (2 V)	7×10^{-7} (1 V) 8×10^{-6} (2 V)	1×10^{-8} (2 V)	2×10^{-6} (1 V) 2×10^{-5} (2 V)	9×10^{-9} (2 V)	2×10^{-7} (2 V)
J (A/cm^2) at 125°C	2×10^{-6} (1 V)	2×10^{-7} (2 V)	6×10^{-9} (1 V) 5×10^{-8} (2 V)	4×10^{-7} (1 V) 1×10^{-5} (2 V)	—	—	1×10^{-7} (1 V) 9×10^{-6} (2 V)	6×10^{-6} (1 V) 9×10^{-5} (2 V)
α (ppm/V^2)	831	2667	1990	—	89	2289	361	460
κ	~15	~20	~18	~30	45	45	~45	~45
Thickness (nm)	10	14	13	16	41	14	40	40

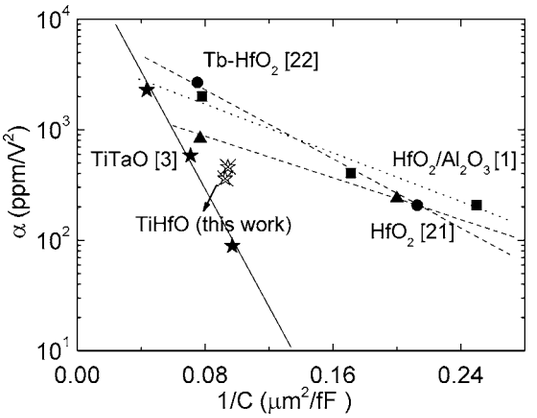

Figure 5. $\Delta C/C$-1/C plots. An exponential decrease of α with increasing dielectric thickness was observed.

higher ϕ_m top electrode and a higher κ dielectric provide a practical approach to achieve low thermal leakage and good VCC simultaneously without reducing the capacitance density, as in a multilayer or laminate structure.

Conclusions

The thermal leakage current in MIM capacitors has been shown to be reduced by work-function tuning. High-performance TiHfO MIM capacitors were developed without sacrificing the overall κ value, which occurs when using a multilayer or laminate structure. This approach improved the voltage-dependent factor α, which is important for analog/RF ICs.

Acknowledgment

This work has been partially supported by NSC (95-2221-E-009-298) and TDPA DOIT MOEA 95-EC-17-A-01-S1-047 of Taiwan.

National Chiao Tung University assisted in meeting the publication costs of this article.

References

1. H. Hu, S. J. Ding, H. F. Lim, C. Zhu, M. F. Li, S. J. Kim, X. F. Yu, J. H. Chen, Y. F. Yong, B. J. Cho, D S. H. Chan, S. C. Rustagi, M. B. Yu, C. H. Tung, A. Du, D. My, P. D. Fu, A. Chin, and D. L. Kwong, *Tech. Dig. - Int. Electron Devices Meet.*, **2003**, 379.
2. S. J. Kim, B. J. Cho, M. B. Yu, M.-F. Li, Y.-Z. Xiong, C. Zhu, A. Chin, and D. L. Kwong, *VLSI Technical Digest*, p. 56–57 (2005).
3. K. C. Chiang, A. Chin, C. H. Lai, W. J. Chen, C. F. Cheng, B. F. Hung, and C. C. Liao, *VLSI Technical Digest*, p. 62–63 (2005).
4. K. C. Chiang, C. C. Huang, A. Chin, W. J. Chen, S. P. McAlister, H. F. Chiu, J. R. Chen, and C. C. Chi, *IEEE Electron Device Lett.*, **26**, 504 (2005).
5. K. C. Chiang, C. H. Lai, A. Chin, T. J. Wang, H. F. Chiu, J. R. Chen, S. P. McAlister, and C. C. Chi, *IEEE Electron Device Lett.*, **26**, 728 (2005).
6. K. C. Chiang, C. C. Huang, A. Chin, W. J. Chen, H. L. Kao, M. Hong, and J. Kwo, *VLSI Technical Digest*, p. 126–127 (2006).
7. C. H. Lai, A. Chin, H. L. Kao, K. M. Chen, M. Hong, J. Kwo, and C. C. Chi, *VLSI Technical Digest*, p. 54–55 (2006).
8. Y. K. Jeong, S. J. Won, D. K. Jwon, M. W. Song, W. H. Kim, O. H. Park, J. H. Jeong, H. S. Oh, H. K. Kang, and K. P. Suh, *VLSI Technical Digest*, p. 222–223 (2004).
9. C. H. Huang, D. S. Yu, A. Chin, W. J. Chen, C. X. Zhu, M.-F. Li, B. J. Cho, and D. L. Kwong, *Tech. Dig. - Int. Electron Devices Meet.*, **2003**, 319.
10. K.-S. Tan, S. Kiriake, M. de Wit, J. W. Fattaruso, C.-Y. Tsay, W. E. Mattthews, and R. K. Hester, *IEEE J. Solid-State Circuits*, **25**, 1318 (1990).
11. *The International Technology Roadmap for Semiconductors*, Semiconductor Industry Association, San Jose, CA (2003).
12. S. B. Chen, J. H. Lai, K. T. Chan, A. Chin, J. C. Hsieh, and J. Liu, *IEEE Electron Device Lett.*, **23**, 203 (2002).
13. C. H. Huang, M. Y. Yang, A. Chin, C. X. Zhu, M. F. Li, and D. L. Kwong, *IEEE MTT-S Int. Microwave Symp. Dig.*, **1**, 507 (2003).
14. S. Blonkowski, M. Regache, and A. Halimaou, *J. Appl. Phys.*, **90**, 1501 (2001).
15. C. Zhu, H. Hu, X. Yu, S. J. Kim, A. Chin, M. F. Li, B. J. Cho, and D. L. Kwong, *Tech. Dig. - Int. Electron Devices Meet.*, **2003**, 879.
16. M. A. Lampert and P. Mark, *Current Injection in Solids*, Academic Press, New York (1970).
17. K. Kao and W. Hwang, *Electrical Transport in Solids*, Pergamon Press, New York (1981).
18. D. Lamp, *Electrical Conduction Mechanisms in Thin Insulating Films*, IEEE (1967).
19. Q. Fang, J. Y. Zhang, Z. M. Wang, J. X. Wu, B. J. O'Sullivan, P. K. Hurley, T. L. Leedham, H. Davies, M. A. Audier, C. Jimenez, J. P. Senateur, and W. Boyd, *Thin Solid Films*, **428**, 263 (2003).
20. A. Palil, *Handbook of Optical Constants*, Academic Press, New York (1985).
21. X. Yu, C. Zhu, H. Hu, A. Chin, M. F. Li, B. J. Cho, D.-L. Kwong, P. D. Foo, and M. B. Yu, *IEEE Electron Device Lett.*, **24**, 63 (2003).
22. S. J. Kim, B. J. Cho, M.-F. Li, C. Zhu, A. Chin, and D. L. Kwong, *VLSI Technical Digest*, p. 77–78 (2003).
23. K. C. Chiang, C. C. Huang, A. Chin, G. L. Chen, W. J. Chen, Y. H. Wu, and S. P. McAlister, *IEEE Trans. Electron Devices*, **53**, 2312 (2006).
24. S. J. Ding, H. Hu, C. Zhu, S. J. Kim, X. Yu, M. F. Li, B. J. Cho, S. H. Chan, M. B. Yu, S. C. Rustagi, A. Chin, and D. L. Kwong, *IEEE Trans. Electron Devices*, **51**, 886 (2004).